

Non-classical interference between independent sources

J.G.Rarity, P.R.Tapster and R.Loudon

DRA Malvern,

St.Andrews Rd, Malvern,

Worcs., UK, WR14 3PS

(December 2, 2024)

When a one-photon state is mixed with a (separate) weak coherent state at a beamsplitter the probability for seeing one photon in each beamsplitter output approaches zero due to destructive interference. We demonstrate this non-classical interference effect using pulse-gated single photons and weak mode-locked laser pulses.

PACS Nos. 3.65b, 42.50

Entanglement and non-classical interference effects of particles with no previous history in common has been the subject of several recent theoretical studies [1-3]. As well as providing further evidence in support of the conventional view of quantum mechanics the realisation of such experiments will prove the feasibility of entangling the large numbers of quanta essential for quantum computation [4]. Here we perform the simplest experiment capable of showing non-classical interference from independent sources by mixing a one-photon state and a weak coherent state at a beamsplitter. This is essentially a reduced version of a heterodyne experiment designed to show non-local interference first suggested by Tan et al [5]. When the weak coherent state cannot be distinguished from the one-photon state by measurement after the beamsplitter we show that the probability of a coincident detection across the beamsplitter output ports goes to zero. In a comparable experiment using classical beams from independent sources [6] the random phase fluctuations lead to a time varying fringe pattern. In the limit where the time uncertainty (jitter) in detection is much less than the rate of phase drift a similar coincidence suppression will be seen but with reduced visibility due to averaging over the random relative phases. In the experiment we derive a good approximation to a one-photon Fock state by using a pulsed parametric downconversion source emitting time correlated photon-pairs. Detection of one photon of the pair is used to gate detection of its partner [7] to within a time window given by the short time duration of the pump pulse (a few hundred femto-seconds). The pump for parametric downconversion is obtained by frequency doubling a femtosecond pulsed laser. A strongly attenuated component of the original laser beam is used as a weak coherent state. This source has no phase correlation with individual beams of the downconverted light and can be thought of as an independent source. The weak coherent state and one photon state can be made indistinguishable by making their time uncertainty longer than their initial pulse lengths by filtering in a narrowband filter before detection. We can investigate the interference between independent classical pulsed sources in the same experiment by accepting all downconversion events (ignoring the gating).

In figure 1 we illustrate a lossless beamsplitter with amplitude transmission and reflection coefficients $t = |t|e^{i\phi_t}$ and $r = |r|e^{i\phi_r}$. Energy conservation requires $r^*t + rt^* = 0$ and $|r|^2 + |t|^2 = 1$ [8] thus $\phi_t - \phi_r = \pi/2$. The single modes at the input ports $| \rangle_a, | \rangle_b$ of the beamsplitter are populated by creation operators a^\dagger and b^\dagger respectively. Then the beamsplitter transforms a^\dagger and b^\dagger into the creation operators c^\dagger and d^\dagger at the output ports of the beamsplitter [8-10] through $a^\dagger \rightarrow tc^\dagger + rd^\dagger$ and $b^\dagger \rightarrow rc^\dagger + td^\dagger$. Taking a vacuum state at the b -port $|0\rangle_b$ and a number state $|n\rangle_a$ at the a -port we obtain the well known result of a binomial distribution for the probability of finding j photons in the c -mode and $n - j$ photons in the d -mode $P_{cd}(j, n - j) = t^{2j}r^{2(n-j)} n!/(j!(n-j)!)$ This result would be obtained if we took a simple ‘coin tossing’ picture where each input ‘photon’ takes a random output direction independent of all other photons.

This picture becomes invalid when we populate each input with a single photon state

$$|1\rangle_a|1\rangle_b \rightarrow (t^2 + r^2)|1\rangle_c|1\rangle_d + rt\sqrt{2}(|2\rangle_c|0\rangle_d + |0\rangle_c|2\rangle_d). \quad (1)$$

When $|r| = |t| = 1/\sqrt{2}$ (the 50/50 beamsplitter) $t^2 + r^2 = 0$ and the probability of detecting one photon at each output port is zero [8] which is clearly non-classical. Using the simple ‘coin tossing’ picture of beamsplitters this result appears counter-intuitive as there is only one ‘coin’ tossed for each pair. This effect was first seen when the coincident photon pairs created in parametric downconversion were mixed at a beamsplitter [11,12].

Generalising to arbitrary number states at both inputs to the beamsplitter we write

$$|n\rangle_a|m\rangle_b \rightarrow (tc^\dagger + rd^\dagger)^n (rc^\dagger + td^\dagger)^m |0\rangle_c|0\rangle_d / \sqrt{n!m!} \quad (2)$$

$$= \sum_{j=0}^n \sum_{k=0}^m t^{m-k+j} r^{n-k+j} \sqrt{{}^n C_j {}^m C_k} {}^{(j+k)} C_j {}^{(n+m-j-k)} C_{(n-j)} |(j+k)\rangle_c |(n+m-j-k)\rangle_d$$

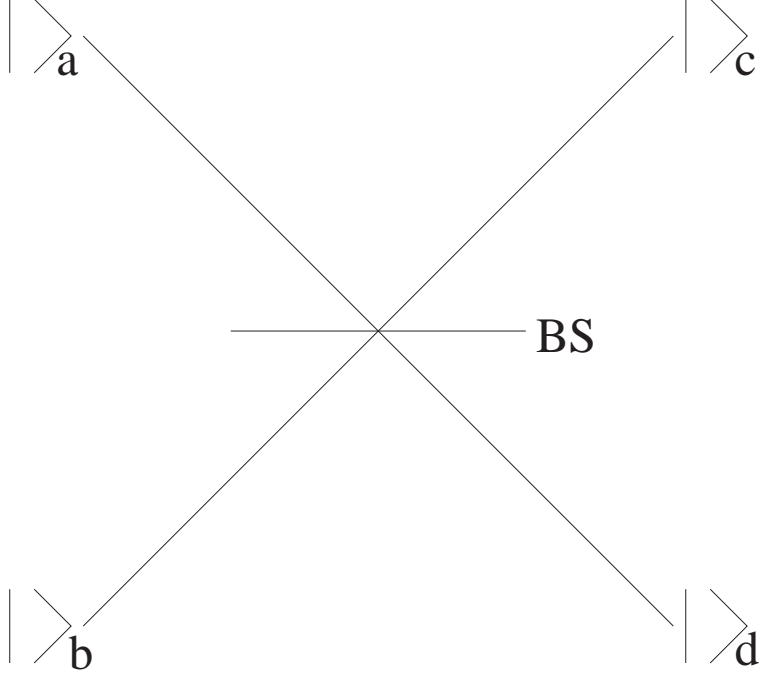


FIG. 1. Overlapping modes at a beamsplitter (BS)

Here we aim to demonstrate interference and thus entanglement between separate sources rather than correlated photon pairs. In the experiment we mix a one photon state with an approximate coherent state $|\alpha\rangle$, where the mean number of photons in the coherent state is $|\alpha|^2$. We can express the coherent state as a linear combination of number states $|\alpha\rangle_a = \exp(-|\alpha|^2/2) \sum_{n=0}^{\infty} \alpha^n / \sqrt{n!} |n\rangle_a$. Applying equation (2) the outputs can be expressed as

$$|\alpha\rangle_a |1\rangle_b \rightarrow \exp(-|\alpha|^2/2) \{ r |1\rangle_c |0\rangle_d + t |0\rangle_c |1\rangle_d + \alpha [(t^2 + r^2) |1\rangle_c |1\rangle_d + rt\sqrt{2} (|2\rangle_c |0\rangle_d + |0\rangle_c |2\rangle_d)] + \alpha^2 [rt^2\sqrt{3} |3\rangle_c |0\rangle_d + t(t^2 + 2r^2) |2\rangle_c |1\rangle_d + r(2t^2 + r^2) |1\rangle_c |2\rangle_d + tr^2\sqrt{3} |0\rangle_c |3\rangle_d] / \sqrt{2} + O(\alpha^3) \} \quad (3)$$

to second order in α .

In the case where the beamsplitter is 50/50 equation 3 again predicts that the probability of seeing exactly one photon in each port of the beamsplitter is zero, independent of α . Realisable photon counting detectors will fire once when they see one or more photons, thus this aspect of the non-classical behavior will be masked when terms in $|n\rangle_c |m\rangle_d$; $n, m > 1$ are present. However these probabilities become negligible as α is reduced to the point where we can ignore powers of α^2 and above.

Realistic detectors are also inefficient. We model detectors with efficiency η as beamsplitters of transmission coefficient η mixing the signal with a vacuum state followed by an unit efficiency detector [13]. As stated above the detectors will fire only once when one or more photons are present thus we have four possible combinations of detections or non-detections with both detectors. For instance if the state reaching the detectors is $|n\rangle_c |m\rangle_d$ we can write these four detection probabilities as

$$\begin{aligned} P_{nm}(0,0) &= (1 - \eta_1)^n (1 - \eta_2)^m \\ P_{nm}(0,1) &= (1 - \eta_1)^n (1 - (1 - \eta_2)^m) \\ P_{nm}(1,0) &= (1 - (1 - \eta_1)^n) (1 - \eta_2)^m \\ P_{nm}(1,1) &= (1 - (1 - \eta_1)^n) (1 - (1 - \eta_2)^m) \end{aligned} \quad (4)$$

The probabilities of obtaining $|n\rangle_c |m\rangle_d$ given by the square moduli of the coefficients in equation (3) can be summed with the above weightings to give the total coincidence probability $P_{tot}(1,1)$. This contrasts with the case where there is no correlation when the a - and b -modes do not overlap at the beamsplitter outputs. Here the probability of seeing a coincidence is just $P_c(1)P_d(1)$ the product of the probabilities of a single count in detectors c and d . This can

be obtained by separate application of binomial partition to the two inputs but also from the equations 4 above ($P_c(1) = P_{tot}(1,0) + P_{tot}(1,1)$ the singles rate is invariant). We define a visibility $V = 1 - P_{tot}(1,1)/P_c(1)P_d(1)$ which measures the fractional reduction of the coincidence rate from its uncorrelated value. This is illustrated as a function of coherent state intensity $|\alpha|^2$ in figure 2. We see the interference visibility rise to near unity as the intensity drops below one photon per pulse.

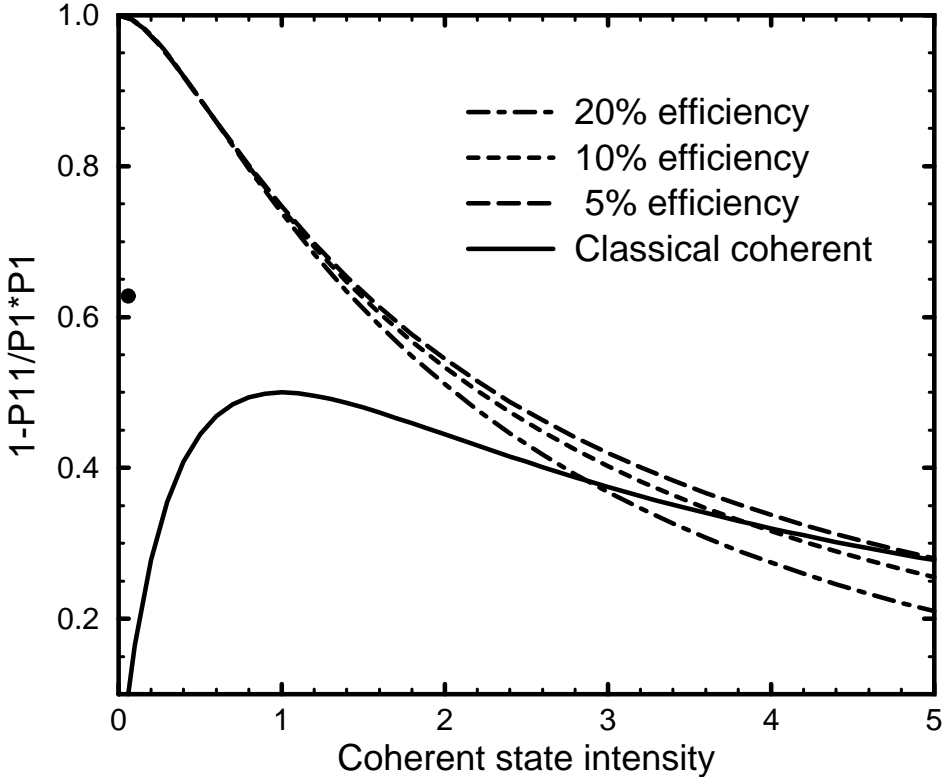


FIG. 2. Interference visibility between a coherent state and a single photon state plotted as a function of the mean number of photons in the coherent state $|\alpha|^2$. Realistic detector efficiencies are taken into account using equations 4. The solid line shows the averaged interference visibility for two random phase classical sources; the horizontal axis then represents R_{ab} and we hold $\langle I \rangle_b$ to be equivalent to one photon per measurement. The experimental result is marked by a \bullet .

We can compare this result with the classical case of two beams of intensity I_a and I_b with randomly varying relative phase ϕ present at the inputs of the beamsplitter. The instantaneous c -mode output intensity is given by

$$I_c = |t|^2 I_a + |r|^2 I_b - 2|r||t|\sqrt{I_a I_b} \sin \phi \quad (5)$$

and similarly in d . When the intensities are low the coincidence rate across the beamsplitter outputs is proportional to the product of output intensities averaged over the random phase ϕ

$$P(1,1) \propto \langle I_c I_d \rangle = |r|^2 |t|^2 (\langle I_a^2 \rangle + \langle I_b^2 \rangle) + (|r|^4 + |t|^4 - 2|r|^2 |t|^2) \langle I_a \rangle \langle I_b \rangle \quad (6)$$

In the interference free case (separate modes) the subtractive term is absent. The interference visibility using constant intensity sources and a 50/50 beamsplitter is thus

$$V = 2R_{ab}/(R_{ab} + 1)^2 \quad (7)$$

where $R_{ab} = \langle I_a \rangle / \langle I_b \rangle$. This is shown in figure 2 for comparison with the non-classical case assuming constant classical intensity. Clearly the visibility reaches a maximum of 50% when $I_a = I_b$.

In both classical and non-classical situations the visibility will be reduced when the mode overlap is incomplete or when the phase fluctuates significantly within the detection time. In previous experiments with separate classical

sources the phase drift was slow due to the narrowband nature of the laser sources and standard detectors (10ns jitter) could be used. Here we limit the detection time jitter by limiting the length of the light pulse itself and use narrowband interference filters to ensure that the coherence time is comparable or longer than this pulse length. We can perform multi-temporal mode analysis of the non-classical interference effect when the coherent state amplitude is small ($\alpha \ll 1$) by extending theory developed in [3,14]. We model the c - and d -mode filters by identical Gaussians with $1/e^2$ intensity (half) width σ and the doubled pump beam as a time-bandwidth-product limited Gaussian pulse with $1/e^2$ intensity width σ_{2P} and assume the gating detector filter is much broader than both. The probability per pulse of a triple coincidence between the gating detector (g) and the c - and d -detectors is then given in the 50/50 beamsplitter case by

$$P(c, d, g) = \frac{1}{2} n_{dc} n_p \eta^3 \left[1 - V \exp \left(\frac{\Delta X^2 \sigma^2}{4c^2(1 + \sigma^2/2\sigma_{2P}^2)} \right) \right] \quad (8)$$

where n_{dc} and n_p ($\ll 1$) are the mean number per pulse of downconverted pairs and weak coherent state photons before the beamsplitter and η^3 is the product of the quantum efficiencies of the three detectors. The coincidence rate as a function of path length difference ΔX shows a Gaussian dip with visibility $V = (1 + \sigma^2/2\sigma_{2P}^2)^{-1/2}$ which is unity when $\sigma \ll \sigma_{2P}$ and falls slowly as σ increases.

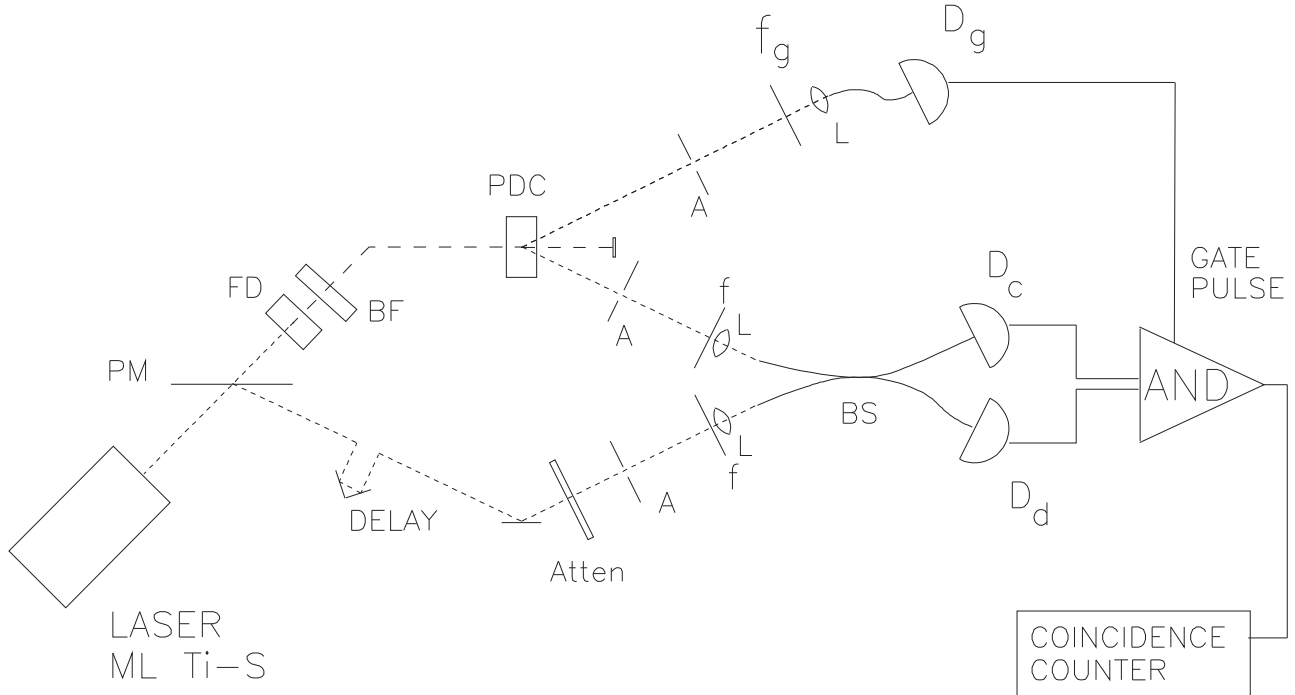


FIG. 3. The experimental apparatus. Key: (ML Ti-S) Mode locked Ti-Sapphire laser, (PM) pick-off mirror, (FD) frequency doubler, (BF) long wavelength blocking filter, (PDC) parametric downconversion crystal, (A) apertures, (Atten) strong attenuator, (f_g , f) interference filters with 815nm centre wavelength, (L) lenses coupling light to optical fibres, ($D_{g,c,d}$) photon counting avalanche photodiodes. Triple coincidences are measured by a gated AND gate. Dotted lines indicate light of 815nm wavelength, dashed lines indicate light of 407.5nm wavelength and thick curved solid lines represent optical fibres.

The experimental apparatus is shown in figure 3. A self mode locked Ti-sapphire laser operating at 815nm centre wavelength ($\simeq 160$ fs pulse length, 100MHz repetition rate) is doubled in a 2mm thick Beta Barium Borate (BBO) crystal. The resulting 407.5nm wavelength pulses are used to pump a 3mm thick BBO crystal with crystal axis tilted to produce a cone of downconverted light around 815nm with half angle $\simeq 7^\circ$. Apertures placed at opposite ends of a cone diameter ensure that we have a near ideal pulsed pair-photon source centred on 815nm. Optical fibres are used to couple this light into photon counting detectors and to further restrict our source to a single mode. Long-wavelength-pass filters are used to ensure that the detectors are not saturated by fluorescence and scatter from the violet pump light. After careful alignment a large proportion of detections are coincident indicating effective detector efficiencies

$>10\%$ [15]. A photodetection in the gate arm of the apparatus is then used to flag the presence of a single photon in the other arm to within the pulse duration. This single photon can then pass into a fibre coupler acting as a 50/50 beamsplitter leading to two fibre coupled detectors (D_c , D_d). Highly attenuated laser pulses are fed into the other input port of the coupler. By using a single mode fibre coupler we ensure that all the detected downconversion and laser light is in a single mode and is indistinguishable after the beamsplitter. To minimise any dispersion effects the fibre pigtail lengths to the coupler are cut equal to within a millimeter. The downconversion pulses and attenuated laser light can then be temporally overlapped by adjusting a variable delay in the laser path length. To further ensure indistinguishability, 3nm bandwidth 815nm filters are placed before each detector fibre. The associated coherence length is then longer than the longest expected pulse duration thus ensuring high visibility interference.

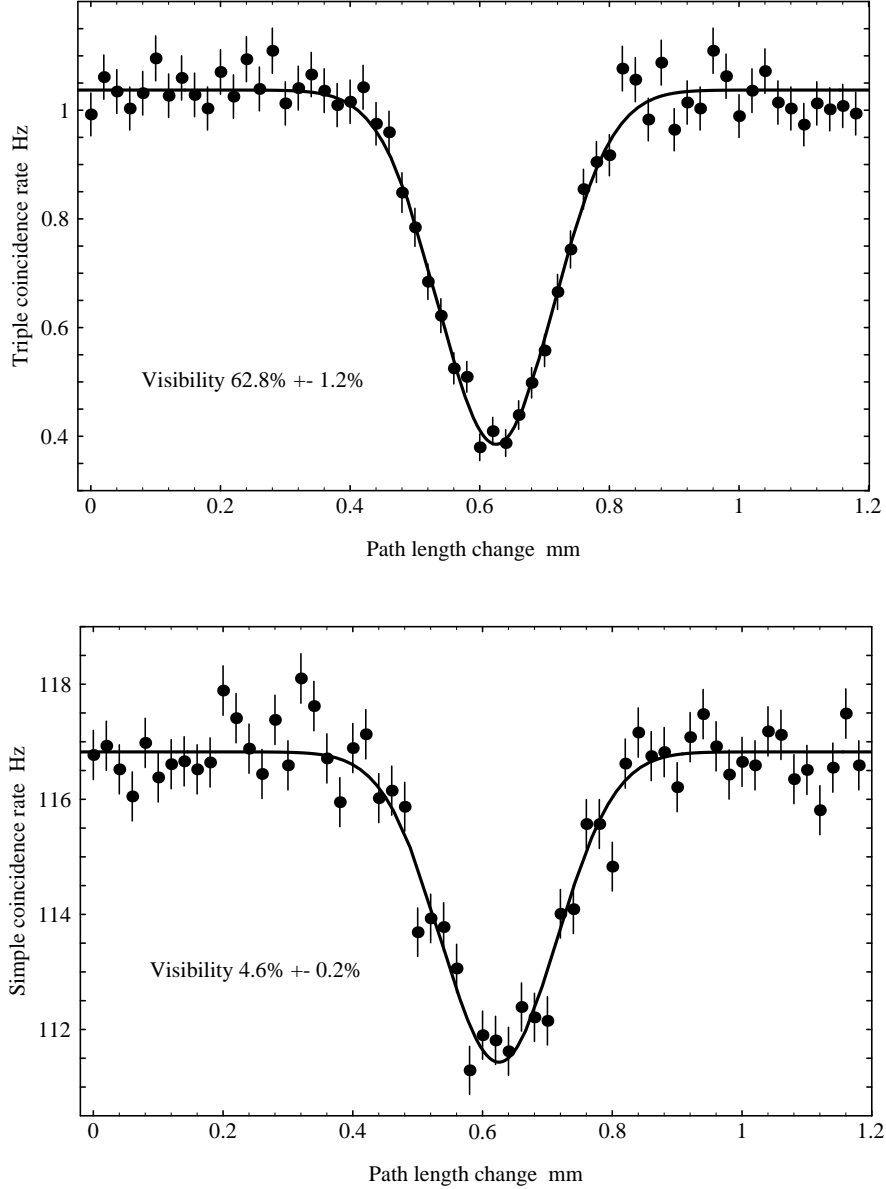


FIG. 4. (a) Triple coincidence rate measured as a function of delay ΔX in the weak laser path. Solid line shows a least squares fit based on the Gaussian function in eq 8 (b) Ungated coincidence rate as a function of delay ΔX .

In the experiment the counting rates due to downconverted photons were of order 5 kilo-counts per second (kcps) while those from the laser were 103 kcps (measured after the beamsplitter by sequentially blocking the laser and downconversion source). The two coincidence rates between between c - and d -mode detectors and the gate detector each were $\simeq 500$ kcps. Doubling these figures to obtain the rates before the beamsplitter allows an estimate of the

triple coincidence rate from equation 8 and the laser repetition rate of 100MHz. This predicts a triple coincidence rate of about 1.1 cps away from overlap. Measuring the coincidences only between *c*- and *d*-mode detectors with the gating bypassed we expect a rate of 117cps if we assume coherent statistics for the filtered mode-locked laser. By simultaneously collecting data with and without the gating active we can compare classical and non-classical interference in the same experiment. In a typical experiment adequate statistics could only be obtained from at least 100 counts per point leading to minimum experiment durations of several hours. Experimental results showing coincidence rates as a function of optical delay are seen in figures 4. Both gated and ungated results show a coincidence reduction at pulse overlap which is well fitted by a Gaussian function of $1/e$ half width $133\mu\text{m}$ (443fs). The visibility of the gated coincidence dip is $62.8\pm1.2\%$ while that for the ungated measurement is $4.6\pm0.2\%$.

This visibility, being greater than 50% is clear evidence of non-classical interference. It is reduced from 100% partly by background triple coincidences from small numbers of pair events arising in the laser and downconversion pulses (about 0.1 events per second). For 3nm full width half maximum bandwidth filters equation 8 suggests we should measure $83\mu\text{m}$ (277fs) $1/e$ half width. This indicates that the pulse length of the downconverted light has been stretched by the walk-off caused by group velocity dispersion in the BBO crystals. This further contributes to reduce the visibility. Initial experiments with a 3mm LiIO₃ crystal (with worse walk-off) showed visibilities of 36% and $200\mu\text{m}$ $1/e$ half width. The visibility of the classical interference is about half that expected from equation 7 using measured count rates (9.2%). We expect that this discrepancy is also due to walk-off effects.

To go beyond this experiment and generate multiparticle interference we will need higher efficiency single photon (Fock) state generators and detectors. Here we are limited to creating much less than one pair photon per mode per pulse in the crystal to minimise the probability of detecting more than one downconversion photon per pulse. The maximum tolerable value will be around $n_{dc} \leq 0.1$ pair-photon per pulse. Similarly our effective detector efficiencies are of order 10% when using single mode fibre. The coincidence rate in an *N*-fold single photon interference/entanglement experiment where each 1-photon state is selected by gating, will scale as $C \simeq Rn_{dc}^N \eta^{2N}$ where *R* is the laser repetition rate. If we gate only one photon as here then this improves to $C \simeq Rn_{dc}^N \eta^{N+1}$. This exponential reduction of rate with increasing *N* is the main factor limiting the further development of quantum computers as it balances any exponential increase in throughput.

In conclusion have shown here that when we take two seemingly separate particles and mix them in such a way that they become indistinguishable then we will see interference effects that are manifestly non-classical.

We acknowledge helpful discussions with Prof F De Martini, Dr H Weinfurter and D Wardle during the preparation of this work.

[1] B.Yurke and D.Stoler, Phys. Rev. Letts. **68** 1251 (1992).
[2] A.Zeilinger, A.Ekert and H.Weinfurtur, Phys. Rev. Letts. **71** 4287 (1994).
[3] J.G.Rarity, in 'Fundamental Problems in Quantum Theory', Ann. New York Acad. Sci. **755**, 624 (1995)
[4] P.W.Shor, in *Proceedings of the 35th Annual Symposium on the Foundations of Computer Science*, edited by S. Goldwasser (IEEE Computer Society Press, Los Alamitos, CA, 1994), p124.
[5] S.M.Tan, D.F.Walls and M.J.Collect, Phys. Rev. Letts. **66**, 252-255 (1989).
[6] R.L.Pfleegor and L.Mandel, Phys. Rev. **169**, 1084 (1967).
[7] J .G.Rarity, P.R.Tapster and E Jakeman, Opt. Commun. **62**, 201 (1987).
[8] H.Fearn and R.Loudon, Opt. Commun. **64**, 485-490 (1987).
[9] Z.Y.Ou, C.K.Hong, and L.Mandel, Opt. Commun. **63**, 118-122 (1987).
[10] R.A.Campos, B.E.A.Saleh and M.C.Teich, Phys. Rev. A, **40**, 1371-1384 (1989).
[11] C.K.Hong, Z.Y.Ou and L.Mandel. Phys. Rev. Lett., **59**, 2044 (1987).
[12] J.G.Rarity and P.R.Tapster, in 'Photons and Quantum Flutuations', E R Pike and H Walther eds., p122. Adam Hilger, London (1988); J Opt Soc Am B, **6**, 1221 (1989).
[13] H.P.Yuen and J.H.Shapiro, IEEE Trans. Inf. Theory, **IT-26**, 78 (1980).
[14] J.G.Rarity and P.R.Tapster in preparation.
[15] J.G.Rarity, P.R.Tapster and K D Ridley, Applied Optics **26**, 4616 (1987).